AD-A143 173 AN ANALYTICAL EVALUATION OF SPALL SUPPRESSION OF IMPULSIVELY LOADED ALUMI..(U) NAVAL POSTGRADUATE SCHOOL MONTEREY CA M K ASADA MAR 84 1/1

UNCLASSIFIED F/G 20/11 NL

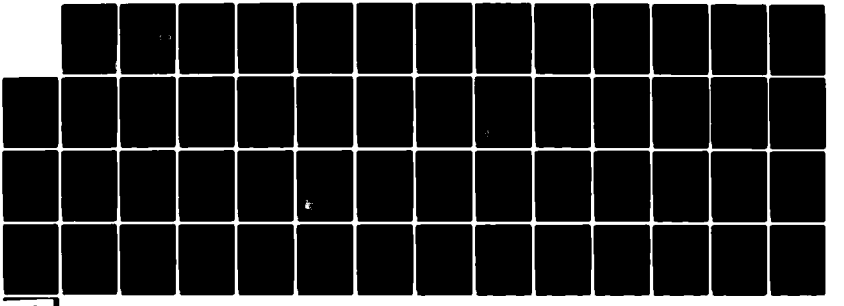

END
DATE FILMED
8-84
DTIC

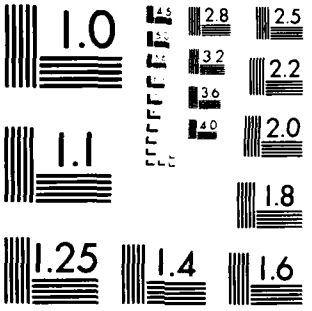

(2)

NAVAL POSTGRADUATE SCHOOL
Monterey, California

THESIS

AN ANALYTICAL EVALUATION OF SPALL SUPPRESSION OF IMPULSIVELY LOADED ALUMINUM PANELS BASED ON A ONE DIMENSIONAL STRESS WAVE PROPAGATION MODEL

by

Michael K. Asada

March 1984

Thesis Advisor: Y. S. Shin

Approved for public release; distribution unlimited.

SECURITY CLASSIFICATION OF THIS PAGE (When Data Entered)

REPORT DOCUMENTATION PAGE		READ INSTRUCTIONS BEFORE COMPLETING FORM
1. REPORT NUMBER	2. GOVT ACCESSION NO. A143173	3. RECIPIENT'S CATALOG NUMBER
4. TITLE (and Subtitle) An Analytical Evaluation of Spall Suppression of Impulsively Loaded Aluminum Panels Based on a One Dimensional Stress Wave Propagation Model		5. TYPE OF REPORT & PERIOD COVERED Master's Thesis March 1984 6. PERFORMING ORG. REPORT NUMBER
7. AUTHOR(s) Michael K. Asada		8. CONTRACT OR GRANT NUMBER(s)
9. PERFORMING ORGANIZATION NAME AND ADDRESS Naval Postgraduate School Monterey, California 93943		10. PROGRAM ELEMENT, PROJECT, TASK AREA & WORK UNIT NUMBERS
11. CONTROLLING OFFICE NAME AND ADDRESS Naval Postgraduate School Monterey, California 93943		12. REPORT DATE March 1984 13. NUMBER OF PAGES 53
14. MONITORING AGENCY NAME & ADDRESS(if different from Controlling Office)		15. SECURITY CLASS. (of this report) Unclassified 15a. DECLASSIFICATION DOWNGRADING SCHEDULE

16. DISTRIBUTION STATEMENT (of this Report)

Approved for public release; distribution unlimited.

17. DISTRIBUTION STATEMENT (of the abstract entered in Block 20, if different from Report)

18. SUPPLEMENTARY NOTES

19. KEY WORDS (Continue on reverse side if necessary and identify by block number)

spall, spallation, spalling, elastic wave propagation, behind armor debris, spall suppression, impulsive loading conditions, shock waves

20. ABSTRACT (Continue on reverse side if necessary and identify by block number)

The response of materials to intense impulsive loading is quite complex. For this reason, an approximate analytical method is used based upon a one dimensional elastic shock approach to analyze the effects of a shaped charge against aluminum panels. This method allows concentration on one aspect of spalling by introducing simplifying assumptions into the governing equations of continuum physics. Then with this information, means to

DD FORM 1 JAN 73 1473 EDITION OF 1 NOV 65 IS OBSOLETE
S/N 0102-LF-014-6601

SECURITY CLASSIFICATION OF THIS PAGE (When Data Entered)

20. ABSTRACT (Continued)

suppress the spall can be developed in order to design or modify an armored vehicle configuration to withstand the catastrophic effects of spallation against its crew members. This work provides a broad overview of stress wave effects in aluminum panels that are caused by rapidly applied loading conditions, together with fundamental results involving elastic shock waves. Results are presented that are useful in obtaining a quantitative appreciation of the behavior of the aluminum under short duration loading. These results may serve as precursors to more complete analyses such as predicting the amount of deformation or spall a specified target experiences when attacked by a certain type of shaped charge.

Approved for public release; distribution unlimited.

An Analytical Evaluation of Spall Suppression of Impulsively Loaded Aluminum Panels Based on a One Dimensional Stress Wave Propagation Model

by

Michael K. Asada
Captain, United States Army
B.S., United States Military Academy

Submitted in partial fulfillment of the requirements for the degree of

MASTER OF SCIENCE IN MECHANICAL ENGINEERING

from the

NAVAL POSTGRADUATE SCHOOL
March 1984

Author: 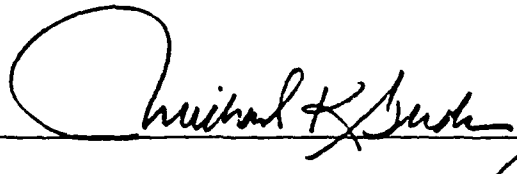

Approved by: 
Thesis Advisor

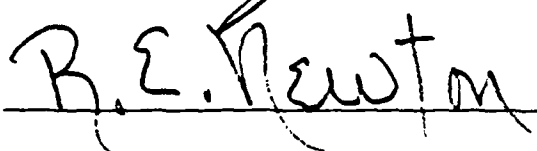
Second Reader

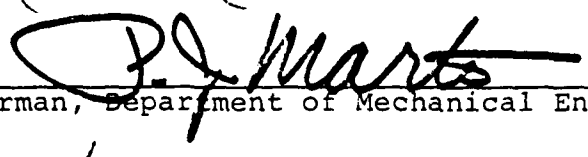
Chairman, Department of Mechanical Engineering

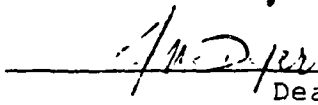
Dean of Science and Engineering

ABSTRACT

The response of materials to intense impulsive loading is quite complex. For this reason, an approximate analytical method is used based upon a one dimensional elastic shock approach to analyze the effects of a shaped charge against aluminum panels. This method allows concentration on one aspect of spalling by introducing simplifying assumptions into the governing equations of continuum physics. Then with this information, means to suppress the spall can be developed in order to design or modify an armored vehicle configuration to withstand the catastrophic effects of spallation against its crew members. This work provides a broad overview of stress wave effects in aluminum panels that are caused by rapidly applied loading conditions, together with fundamental results involving elastic shock waves. Results are presented that are useful in obtaining a quantitative appreciation of the behavior of the aluminum under short duration loading. These results may serve as precursors to more complete analyses such as predicting the amount of deformation or spall a specified target experiences when attacked by a certain type of shaped charge.

TABLE OF CONTENTS

ACKNOWLEDGMENT

The author wishes to express his sincere gratitude to those who assisted him in the preparation of this work. In particular, he is very grateful to Professor Young S. Shin for his active interest and continued support in this research work.

The author also wishes to thank Mr. Ronald E. Musante, Mr. Anthony P. Lee and the staff of FMC Corporation's Ordnance Division for their cooperation and assistance in this project. Without their provisions of range facilities, ammunition and materials, this study would not have been possible.

In addition, the author is grateful to Colonel Robert M. Wilson, Mechanics Department Head, United States Military Academy and Colonel David H. Cameron, Mathematics Department Head, United States Military Academy, for their continued support during the early academic period. Their untiring active efforts provided the inspiration to persevere and achieve many personal and professional goals.

Finally, truly unbounded thanks are due to the author's family, who with their love and patience supported him during his quest for higher learning.

I. INTRODUCTION

In order to determine whether or not methods to suppress the behind armor effects caused by shaped charges against armored vehicles provide reliable and accurate predictions, it is essential that they be evaluated by carrying out detailed experiments in order to obtain experimental data that can be analyzed. It is for this purpose that the present experiment was performed.

In particular, experimental data is sought to provide information on permanent deformation as well as detailed transient strain on simple structures which actually undergo three dimensional structural deformations when subjected to planar impulsive loads. However the scope of this analysis is confined to one dimension in order to convey elegantly the effects of the longitudinal stress wave that is propagated through the structure and to propose an effective way to suppress the amount of damage. Accordingly, square panels of 5083 aluminum armor were prepared and subjected to detonations from a 3.2 inch high explosive shaped charge located at the midpanel. Two configurations employing kevlar as a spall liner were tested to determine the optimal system in suppressing the behind armor effects. Nominally on each of the three specimens, six strain gages were affixed at prescribed stations and transient strain records

were recorded by the surviving gages. It was intended that the resulting strain data be converted to stresses and then compared to theoretical fracture stresses for the aluminum panels. By employing transient strain data to compare with theoretical values of fracture stresses, it is intended to assess whether or not the approximate impact interaction model being used is adequate and, if not, to gain indications of aspects requiring improvement so that appropriate modifications and improvements can be carried out for future spall predictions.

II. NATURE OF THE PROBLEM

A. BACKGROUND LITERATURE

The desirability and survivability of U.S. armored fighting vehicles on today's modern battlefield has been under intense criticism since the close of World War II and most notably in recent years. This was especially highlighted by the rather large percentage of losses that occurred on both sides in the October 1973 Arab-Israeli war. Yet despite these facts, it does not eliminate the need to maintain a technology to build and improve the survivability of combat vehicles.

Tanks and Armored Personnel Carriers (APC's) were born from a long term need for a land-based system that combined firepower, protection and mobility. The basic concept was demonstrated long ago in the war chariots of ancient civilizations and the armor-clad knights of the middle ages [Ref. 1].

However if one questions the role and survivability of these modern armored fighting vehicles (AFV's), then one should first question the survivability of a man, a manportable weapons system, or an unprotected (unarmored) weapons platform in the environment of modern blast, fragment, nuclear, chemical and biological weapons. A basic feature of the fighting vehicles is that it raises the threshold of

weapon capability required to injure a human by requiring the weapon to first defeat the armored envelope. But with the advent of the weapons utilizing the shaped charge, the requirement to defeat the armor became much easier. In fact, the capabilities of the shaped charge enable it to penetrate "any known armor."

B. THEORY OF SHAPED CHARGE AND JET PENETRATION

A shaped charge weapon consists essentially of a hollow liner of inert material, usually metal, and of conical, hemispherical, or other shape, backed on the convex side by

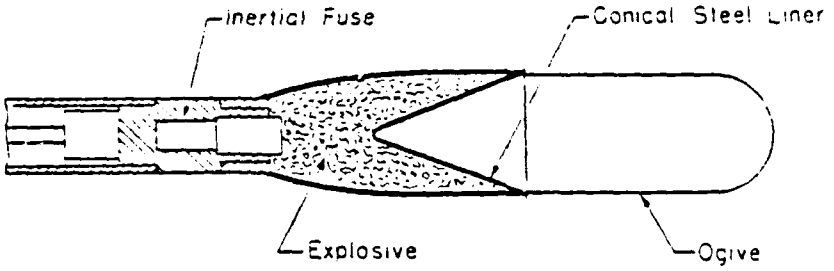

Figure 2.1 Schematic of Shaped Charge Configuration

an explosive as shown in Figure 2.1. Figure 2.1 shows a cross sectional view of the head of a Soviet RPG-7 (rocket propelled grenade) which contains a typical conventional hollow charge. When this weapon strikes a target, the base fuze, operating on the inertia principle, detonates the charge from the rear. A detonation shock wave travels

forward and collapses the conical liner, starting at its apex. The collapse of the cone squirts forward a long, narrow jet of copper at approximately 25,000 feet per second [Ref. 2]. This process is illustrated by the series of high-speed radiograph photographs as shown in Figure 2.2. The photographs are arranged to show the sequence of events in one charge. The last picture shows a jet perforating an armor plate. Early in the process of its formation, the jet breaks up into fine particles but retains its jetlike characteristics out to great distances. There is a gradient to the velocities of the particles along the jet, the particles

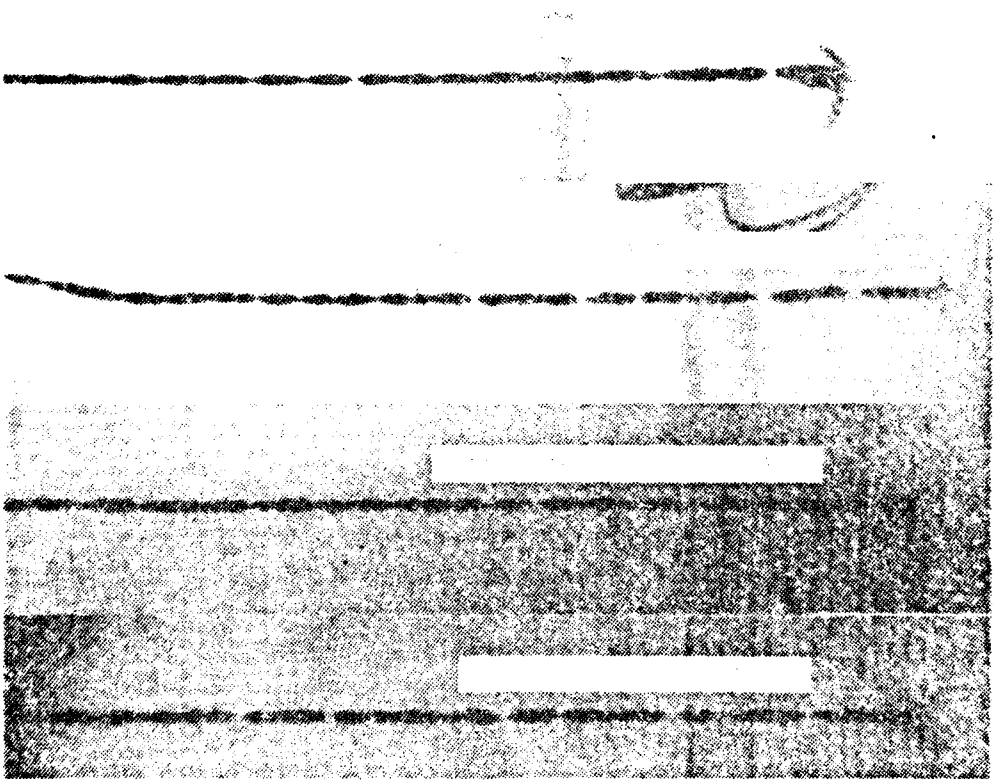

Figure 2.2 High-Speed Radiograph of Shaped Charge (Photo courtesy of FMC)

in front moving faster than those at the rear [Ref. 3]. This causes the jet to lengthen and reduces its average density with time. When a jet strikes a target of armor plating, intense pressures are produced at the point of contact. These pressures are so far above the yield strength of the armor material that the target flows out of the path of the jet as would a liquid.

Since the pressures produced by the jet are much greater than the yield strengths of most target materials, both the target and the jet can be considered as fluids in calculating the depth of jet penetration. Simple hydrodynamic analysis can be used to approximate the depth of jet penetration. The point of contact of a fluid jet with the target moves through the target at a velocity u. If the jet has an absolute velocity v, its velocity relative to this point is v-u. The pressure at this point due to the jet is the same as that due to the target material, which has relative velocity u toward this point. Thus by Bernoulli's theorem:

$$\tfrac{1}{2}\rho_j(v-u)^2 = \tfrac{1}{2}\rho u^2 \qquad \text{(Eqn 2.1)}$$

or

$$\frac{u}{v-u} = \sqrt{\frac{\rho_j}{\rho}} \qquad \text{(Eqn 2.2)}$$

where ρ_j is the density of the jet and ρ is the density of the target material. But primary penetration T equals

the penetration velocity u times the time of penetration, $1/(v-u)$

or

$$T = \frac{ul}{v-u} = l\sqrt{\frac{\rho_j}{\rho}} \qquad \text{(Eqn 2.3)}$$

where l is the length of the jet.

The theoretical basis for this formula assumes a number of things such as the pressure exerted by the jet remains high enough for the target to behave as a fluid, and that the target material pushed to the sides of the crater remains there so that it does not have to be rehit (fluid streamline geometry) [Ref. 4]. In light of this formula, a jet of higher density, such as gold, will penetrate deeper than that of lower density, such as copper, if the jets have the same length. Since the ductile, high-density materials such as gold, platinum and the like are rather expensive, the usual material used for shaped charges liners is a soft ductile pure copper.

C. BEHIND ARMOR EFFECTS PRODUCED BY SHAPED CHARGES

As a jet pierces a target plate, it produces a small cloud of spall particles from the rear surface of the plate as shown in Figure 2.3. These particles travel off the back of the plate in an expanding cloud that looks just like the cloud of earth and rock that one makes when exploding a shallowly buried charge in an open field. The spall debris

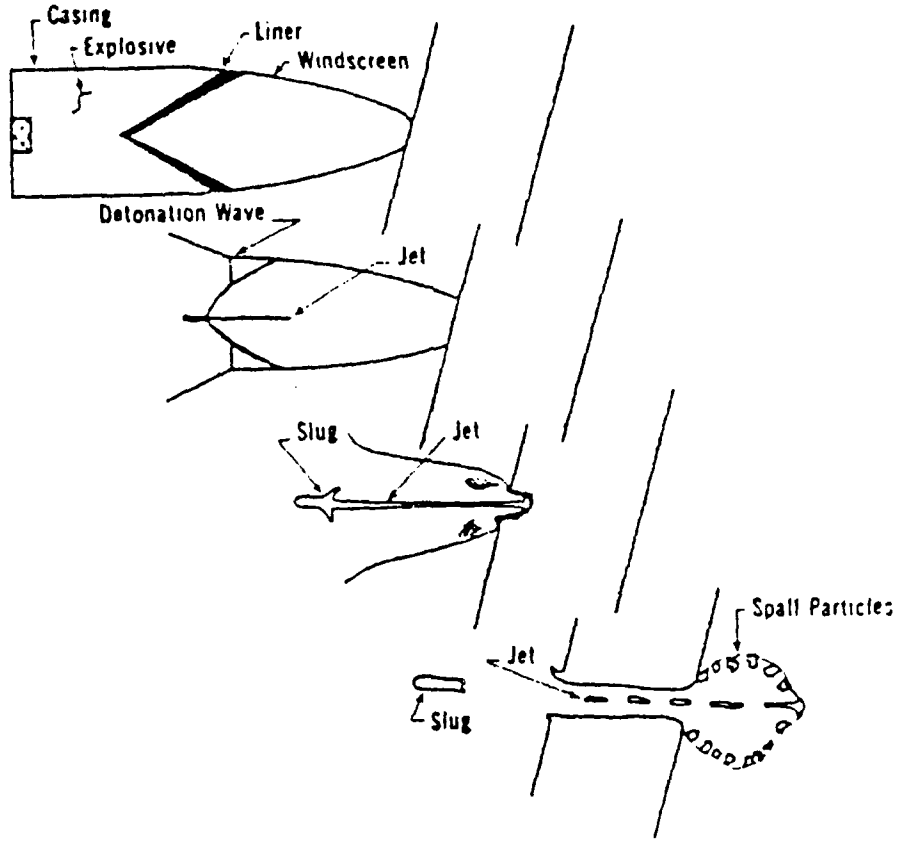

Figure 2.3 Shaped Charge Functioning and Target Defeat [Ref. 7]

travels about the interior of the AFV along with the particles formed from the remainder of the jet. The separated layers of material leave behind a spall ring on the rear surface of the armor as shown in Figure 2.4. In general, the spall particles have a lower velocity than the jet

Figure 2.4 Rear Spall Ring if 1-3/4 inch Aluminum Armor

particles and cause less damage; but they can still be deadly to crew members and some equipment. In the particular use of aluminum armor, however, the spall particles can sometimes cause a devastating effect.

The phenomenon of spalling can best be analyzed when one observes what actually happens at the moment of the shaped charge detonation. As the high explosive shaped charge is detonated in direct contact with a slab of material, the

explosive undergoes a rapid transformation. This quick change from a solid to a gas releases great quantities of energy so quickly that a high pressure pushes against the material. This high pressure moves through the material rapidly in the form of a shock wave that can cause the material to deform or fracture if the pressures and reflections from other surfaces are great enough. If the target is sufficiently thin a puncture will result. If the target is relatively thick, the shock wave will propagate through the material and reflect from a parallel free surface as a rarefaction wave, so that the normal stress will be substantially zero. Hopkinson [Ref. 5] pointed out that such an interaction could result in a net tension behind the free surface, whose value could exceed the ability of the material to maintain its integrity and hence would account for the spalling phenomenon [Ref. 6]. The amplitude of the reflected waves may be of sufficient magnitude to produce fractures near and approximately parallel to the surface. The portion of the target material between the fracture and the rear surface is known as the "spall." The energy trapped in this spall may cause a rear surface bulge; or, if sufficiently great, the material may become detached from the target creating a shrapnel effect. The fracture will be formed if the tensile stress reaches the critical dynamic strength of the target material.

D. SUPPRESSION OF BEHIND-ARMOR EFFECTS

The need to suppress armor spall has long been recognized. Debris ejected from the inside surfaces of wooden ships struck by cannon balls and stone fortifications struck by solid shot emphasized the fact that it became important to protect the occupants from the fragmentation of the armor protection. Therefore an effective way of accomplishing this was to hang curtains behind and away from the wall of fortification. The effectiveness of such shields have been proven in the past as described by Lt. A. D. Wharton of the Confederate Ship Tennessee after being hit by a 15 inch shot from the Union Monitor Manhattan; "Stand clear of the port side ... a moment after, a thunderous report shook us all ... this was the only 15 inch shot that hit us fair. It did not come through, the inside netting caught the splinters, and there were no casualties from it" [Ref. 7].

Thus, although the armor array was usually severely perforated by any charge or projectile, the netting, or spall curtains, caught the behind armor debris that could have caused serious injury to the crew. Hence means to minimize such effects have been sought for many years. Polyethylene was identified in the early 1960's as an effective behind armor spall-suppression material and the use of such materials in AFV's for the attenuation of spall effects is known worldwide [Ref. 8]. Another material suggested in the early 1960's as an interior liner was glass reinforced

plastic (GRP) also known as doron. Doron demonstrates excellent armor qualities and can be used as a primary construction material for the vehicle hull and turret. However, glass reinforced plastic armor has a significant deficiency: when it is penetrated by a shaped charge munition such as a high explosive anti-tank (HEAT) round, a cloud of very high velocity glass particles is produced which can be a severe hazard to the crew's eyes, flesh and lungs.

The search for materials ballistically superior to both GRP and polyethylene has continued. Recent research by the U.S. Army Materials and Mechanics Research Center has proved the value of similar liners of modern materials, such as kevlar, in Armored Personnel Carriers (APC's). The M113A1 APC has, for example, in the course of product improvement testing, been subjected to contact detonation by shaped charges in order to design retrofit armor to upgrade the AFV. Although the penetration holes were large, and the spall production was widespread, experimental spall liners were able to capture the majority of the fragment spray behind the armor. As a result of the pioneering demonstrations by FMC Corporation in late 1974, the Army became interested in Dupont's proprietary filament "kevlar," particularly for use behind aluminum armor. Kevlar is a high modulus, aromatic fiber, and in an appropriate matrix and weave, has been demonstrated to be a superior spall

liner material. The early ballistic tests performed by FMC demonstrated that about 1/2 inch thickness of the kevlar material placed behind the APC aluminum armor captured more than 90% of the spall fragment spray produced by a statically detonated shaped charge [Ref. 9].

Although the current research and development program to develop spall-suppression liners for aluminum armored fighting vehicles such as the M113A1 as shown in Figure 2.5 have proven successful, the actual problem of the spallation

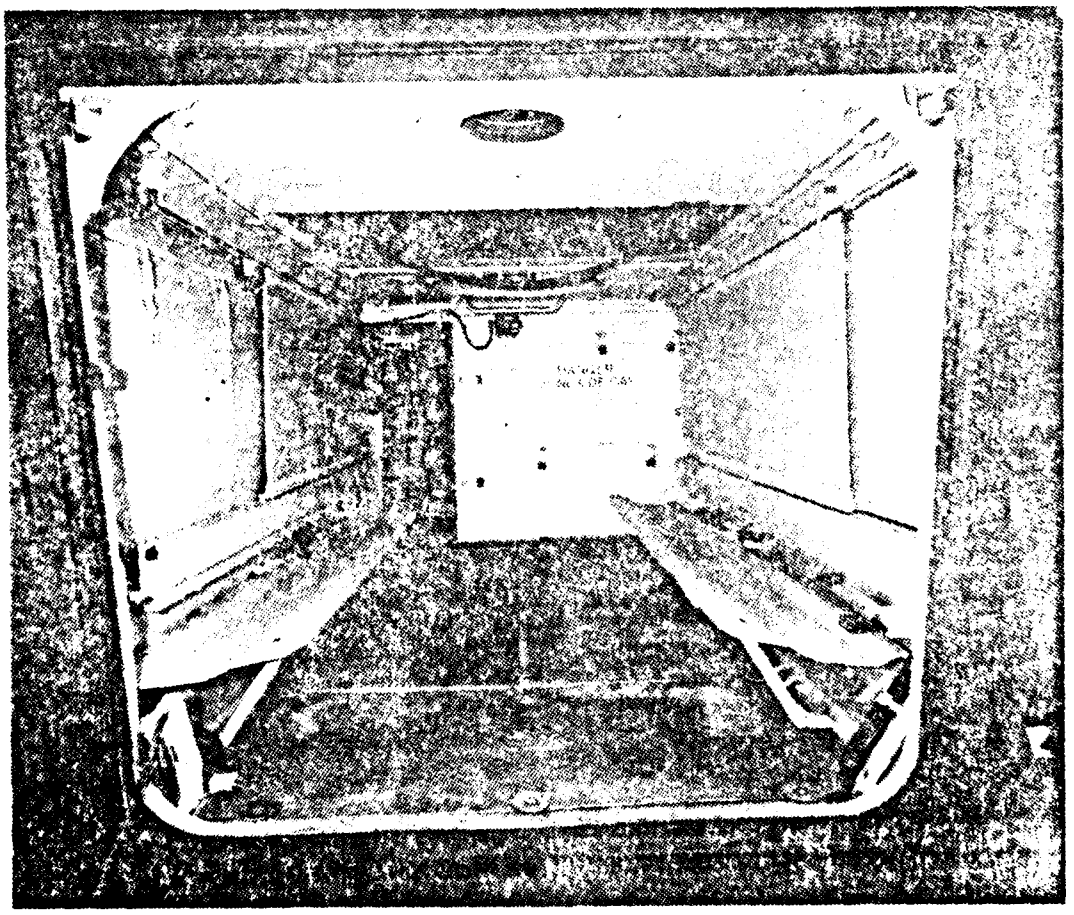

Figure 2.5 M113A1 with Spaced Kevlar Liner
(Photo courtesy of FMC)

of the armor material has been neglected. The spall curtains incorporated by FMC are as stated, a retrofit method to capture the existing spall and behind armor debris caused by a shaped charge. As is, the spall liners do not actually reduce the amount of spall that occurs. Instead this after the fact suppression technique accepts that the spall will occur and the problem is to attenuate the effects of the spallation. What is actually needed and proposed in this study is an attempt to incorporate analytical methods to determine suppression techniques and then confirm it by extended experimentation.

III. EXPERIMENTAL ARRANGEMENT AND PROCEDURE

A. TEST SET UP

Since the static performance of a shaped charge always equals or surpasses its performance when fired dynamically, it was decided to start the search for techniques of spall suppression by using a small charge that would simulate a round being fired from a Soviet shoulder fired weapon and one that could be detonated statically. Although liners of various shapes and materials could have been used, the Ballistic Research Laboratory (BRL) 3.2 inch precision shaped charge employing a copper cone liner (60 degree cone angle with octol explosive-75/25 TNT) was adopted because this shaped charge is considered a reproducible simulant for the Soviet RPG-7.

The experiment was devised with two purposes in view: first, to obtain permanent deformation experimental data (depth of spall) in order to determine the effectiveness of the suppression system employed; and second, to obtain a transient response of strain to investigate the fundamental laws governing the shock wave propagation process (magnitude of stresses).

To meet these objectives, an initially flat square panel (24 x 24 in.) of welded 5083 aluminum armor plate (1-3/4 in. thick) impulsively loaded by a static shaped charge was

chosen. The test occurred at the FMC Hollister Test Facility. For the static test, the projectile was held in position at the required obliquity (0 degrees for this test) against the target and detonated. (Reference Figure 3.1)

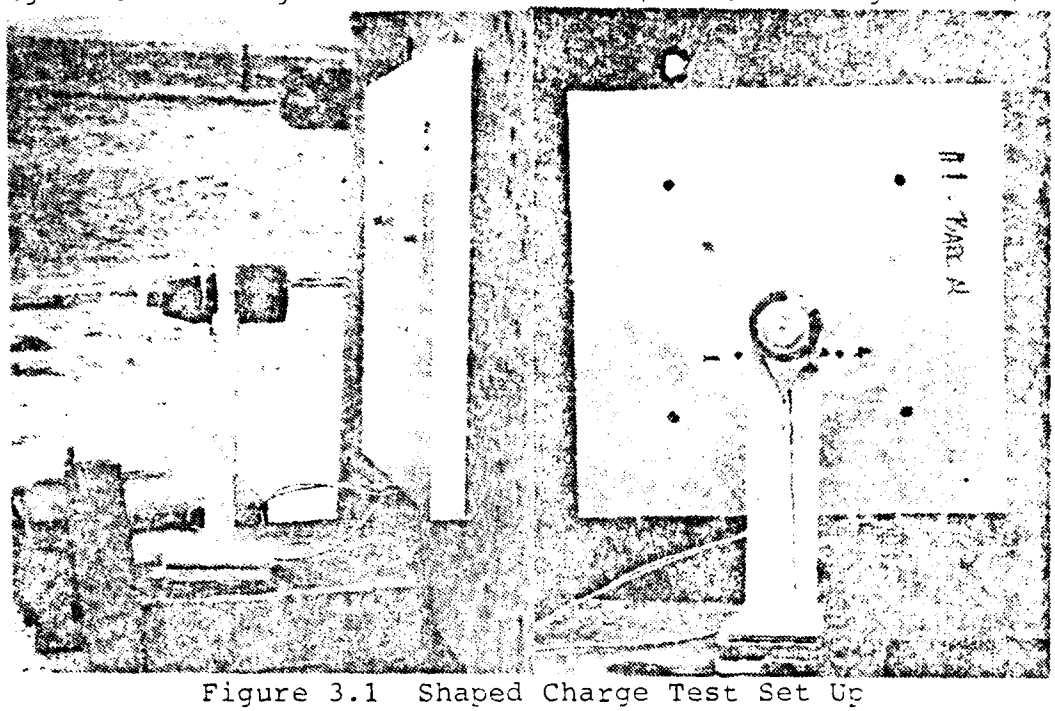

Figure 3.1 Shaped Charge Test Set Up

A large steel base plate with a vertical blast shield (2 in. x 8 ft. x 3 ft.) welded onto the base, with supports of 3 inch x 5 inch rectangular steel tubing comprise the test stand. (Reference Figure 3.2 and Figure 3.3) The shaped charges rest in a wooden cradle placed 8 inches from the front surface of the 5083 aluminum armor. With contact armor configurations, the kevlar liner was placed in direct contact with the back of the aluminum panel and then rested against the blast shield. For spaced armor systems, the kevlar liner was displaced from the back of the aluminum

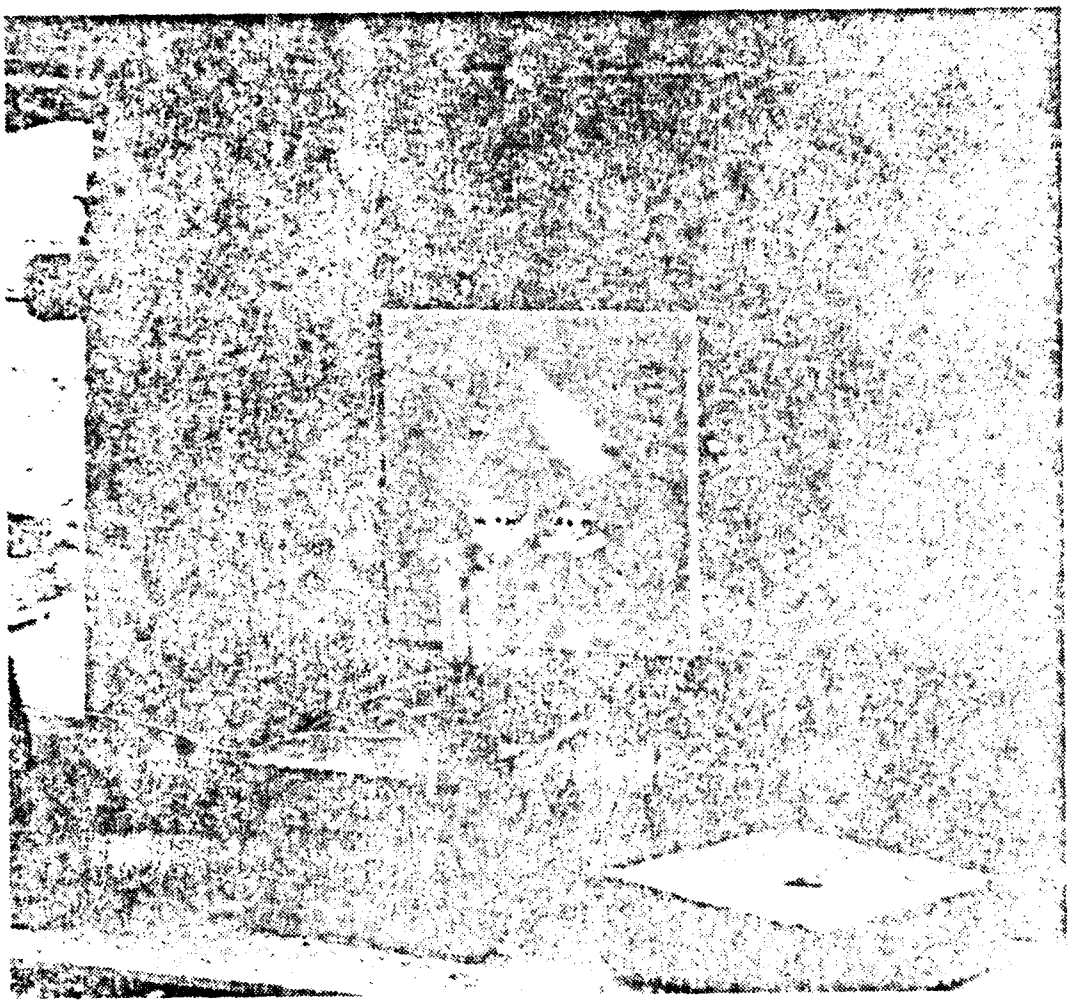

Figure 3.2 Front View of Test Stand

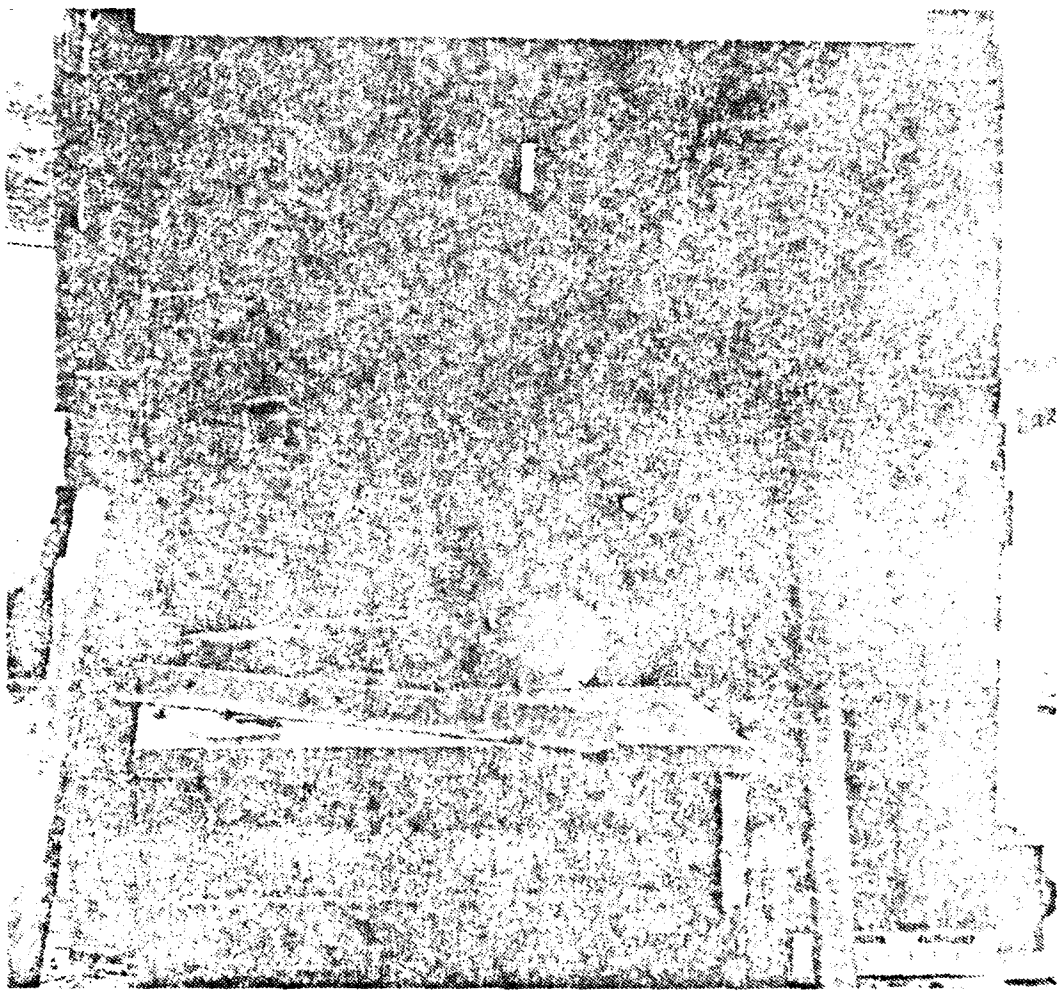

Figure 3.3 Rear View of Test Stand

panel by an 8 inch air gap as shown in Figure 3.4. A high speed camera was also set up behind and away from the explosion in order to record the event.

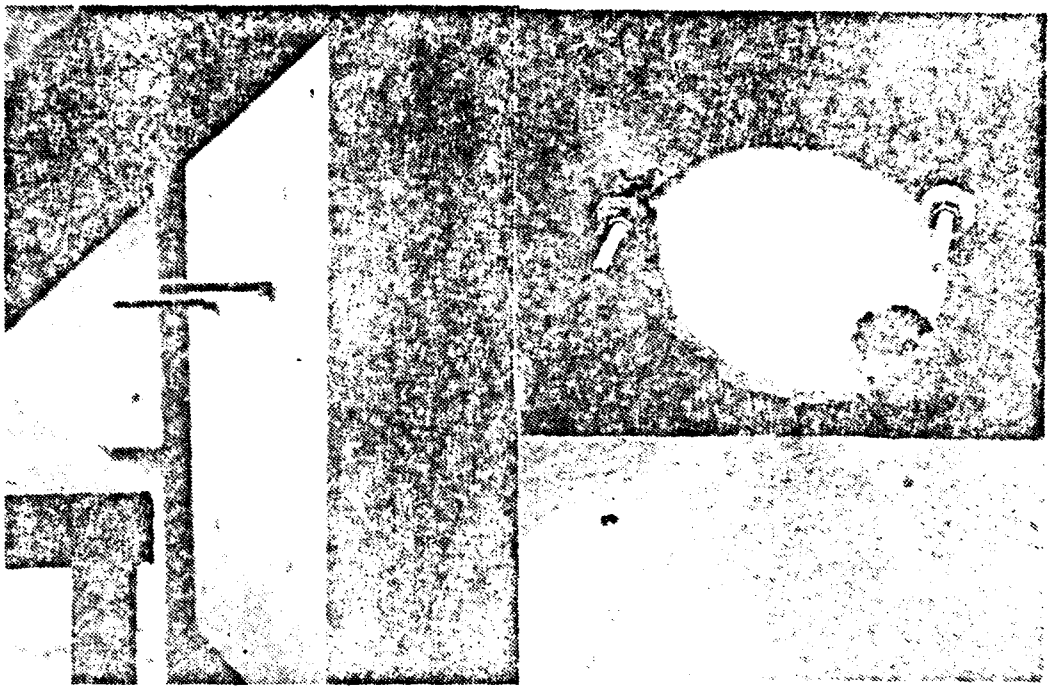

Figure 3.4 Kevlar Liner Configurations

B. TEST PROCEDURE

The aluminum panel specimens were bolted to the heavy steel blast shield. The shaped charge was centered at the midwidth-midspan point. As the shaped charge was detonated, the elastic shock wave proceeded longitudinally and radially from this initiation point, resulting in a stress wave propagation that occurred almost simultaneously.

Three shots employing basically the same test set up were fired. The firing sequence is entered in Appendix A

which describes the conditions established for each of the three shots. Shot #1 was the calibration shot designed to calibrate the recording devices used to measure the transient strain. Shot #2 was designed to see what effects a direct mounting of the kevlar liner to the back of the aluminum panel would have in suppressing the degree of spall. Shot #3 was designed to see what effects an air gap between the kevlar liner and the back of the aluminum panel would have in suppressing the projection of spall.

C. INSTRUMENTATION

In an effort to measure transient strains, type SR-4 foil type strain gages were oriented and attached at various locations on the front and back surface of the aluminum panel as listed in Table A.2 (see Appendix A). These gages were attached with Eastman 910 cement and cured as advised by the manufacturer. Each transient strain gage was fed to a standard wheatstone bridge and the strain signal was recorded on a Honeywell recorder. Because none of the strain gages survived the effects of the blast, no permanant strain traces were able to be recorded.

Since appropriate photographic or other equipment for measuring or recording transient deformation of structures was not available, only post-test configuration measurements have been obtained for these specimens. Each panel had its front and back surfaces machined flat and parallel to facilitate the depth of spall measurement.

D. TEST RESULTS

After each test shot, all three panels experienced an extreme degree of permanent deformation with an observed back spall ring of approximately 3-1/2 inches in diameter as shown in Figure 3.5. Because the boundary conditions are

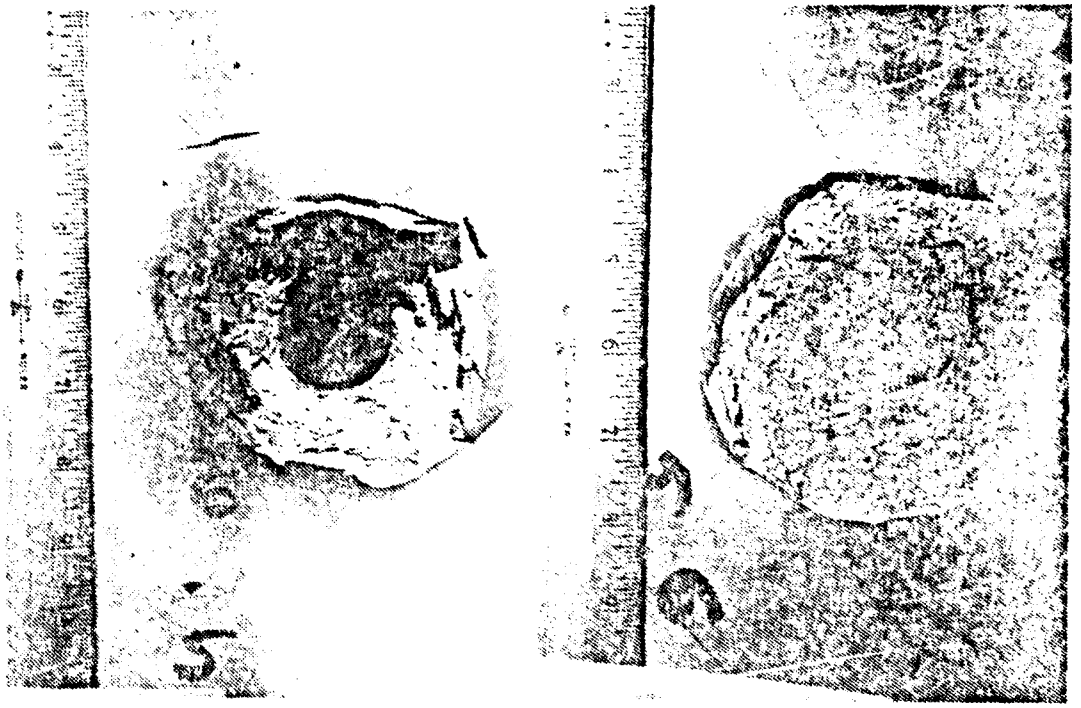

(A) (B)

Figure 3.5 (A) Displaced Kevlar (B) Mounted Kevlar

the same for shot #1 and shot #3 (i.e., free surface on back side of panel), the spall pattern is identical. However for shot #2, there is an obvious reduction in the amount or depth of spall due to the kevlar liner system mounted directly in contact with the back side of the aluminum armor. In particular, for shots #1 and #3, the depth of spall was approximately 0.47 inches and for shot #2, the

depth was 0.28 inches. It appears that the test results for permanent deformation are consistent with the theoretical development of spall suppression discussed in chapter 4. Although the spaced kevlar liner configuration of shot #3 appeared to capture a large portion of the spall debris resulting from the impulsive loading and possibly even reduce the cone angle of the spall fragments, the obvious conclusion is that this method of spall suppression is an after the fact remedy aimed at arresting the existing spall from dispersing and not at reducing the amount of spall. Because the specimen geometry and material properties, the loading conditions and the permanent deformation data are sufficiently well defined, it is believed that the test results provide reliable data for evaluating appropriate prediction models involving implusive loading conditions for future tests.

The locations of each of the strain gages for which transient strain measurements were attempted are given in Appendix A. As mentioned the recording of the event by the Honeywell recorder was then passed through the HP 5451C Fourier analyzer which converted the signal into a time history of the transient strain. The strain traces were calibrated accordingly.

In general, certain strain traces appeared throughout the recorded time history, while others vanished after a short time (probably because of broken lead wires), and

still others reflected essentially zero strain after apparently behaving in a plausible fashion for an initial period. In this latter case, it is likely that the strain gage became detached from the panel after a short time. In all cases, post test observations confirmed that all strain gages became detached due to the severe blast effects. Another obvious observation from the strain traces indicated a definite discrepancy with the magnitude of the strain (in volts) and the time axis for all of the graphs. One explanation for this case may be due to the fact that the blast signal could have exceeded the limits of the recorder and saturated the amplifier. Therefore the instrumentation set up was insufficient to give a proper time history representation.

IV. ANALYSIS OF SPALLING AND SPALL SUPPRESSION FROM SHOCK WAVES

A. THEORETICAL BACKGROUND OF TRANSIENT DISTURBANCES

In the vast majority of cases when we solve engineering problems using elasticity, or the strength of materials approach, we use steady state solutions. However in a number of situations, we must consider the transient problem where we must take into account the propagation of elastic waves into the material.

Normally the time it takes to load a body is very long relative to the time it takes elastic waves to travel through the stressed regions and conditions are essentially static. However when the loading is impulsive (i.e., by explosion or high velocity impact), then failures occur which we can not predict by a static analysis (see Figure 4.1).

Figure 4.1 Spalling Phenomenon [Ref. 8]

As we will see, a compressive pulse moves down the rod and reflects from the free end as tension. Brittle materials are much weaker in tension than compression and failure occurs. The same peak stresses applied slowly in compression would not cause failure.

As the simplest case of elastic wave propagation we consider logitudinal motion in a slender rod (this shows many of the features of more complicated geometries). Consider only axial stresses and displacements as shown in Figure 4.2.

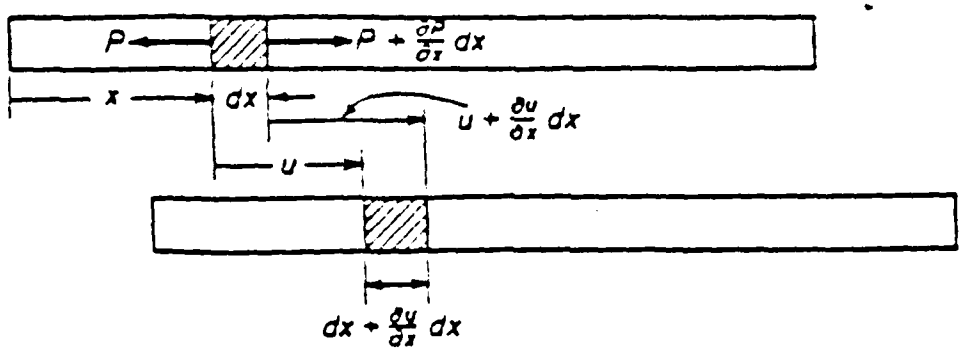

Figure 4.2 Displacement of Rod Element

Consider an element of this rod of length dx as shown in Figure 4.2. If u is the displacement at x, the displacement at x + dx will be $u + \frac{\partial u}{\partial x} dx$. It is evident then that the element dx in the new position has changed in length by an amount $\frac{\partial u}{\partial x} dx$, and thus the strain is $\frac{\partial u}{\partial x}$. Since from

Hooke's law the ratio of stress to strain is equal to the modulus of elasticity E, we can write

$$\frac{\partial u}{\partial x} = \frac{P}{AE} \qquad \text{(Eqn 4.1)}$$

where P is the axial tension and A is the cross-sectional area of the rod. Differentiating with respect to x gives,

$$AE \frac{\partial^2 u}{\partial x^2} = \frac{\partial P}{\partial x} \qquad \text{(Eqn 4.2)}$$

Apply Newton's second law of motion for the element and equate the unbalanced force to the product of the mass and acceleration of the element

$$\frac{\partial P}{\partial x} dx = \rho A dx \frac{\partial^2 u}{\partial t^2} \qquad \text{(Eqn 4.3)}$$

where ρ is the density of the rod, mass per unit volume. Eliminating $\frac{\partial P}{\partial x}$ between equations 4.2 and 4.3, we obtain the partial differential equation

$$\frac{\partial^2 u}{\partial t^2} = \left(\frac{E}{\rho}\right) \frac{\partial^2 u}{\partial x^2} \qquad \text{(Eqn 4.4)}$$

or

$$\frac{\partial^2 u}{\partial t^2} = c^2 \frac{\partial^2 u}{\partial x^2} \qquad \text{(Eqn 4.5)}.$$

The velocity of propagation of the displacement or stress wave in the rod is then equal to

$$c = \sqrt{\frac{E}{\rho}} \qquad \text{(Eqn 4.6)}$$

[Ref. 10].

Equation 4.5 is the one dimensional form of the wave equation where the most general solution is U = F(X - CT) + G(X + CT). This is easily verified by direct substitution as long as F and G are differentiable functions of X. The function F(X - CT) corresponds to a pulse which has shape F(X) at T = 0 and moves in the positive X direction with speed 0 without distorting. Similarly G(X + CT) corresponds to a pulse of shape G(X) at T = T1 which moves in the negative X direction with velocity C without distorting as shown in Figure 4.3.

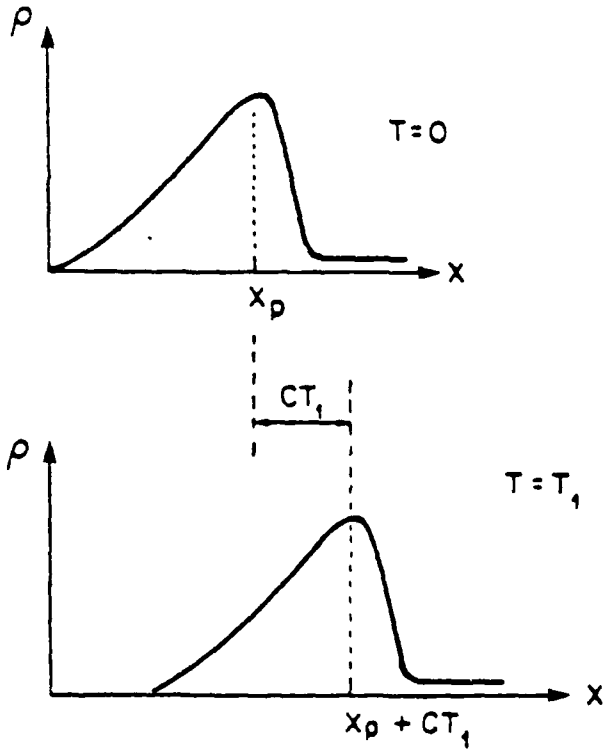

Figure 4.3 Pulse Shape

Because the velocity of an element of material is not the same as the wave velocity, two velocities must be considered. These two velocities are the velocity of propagation c of the disturbance, and the particle velocity v, with which a point in the material moves as the disturbance moves across it (this is similar to water waves, i.e., a piece of wood bobbing on the surface does not move with the wave velocity).

Refer to Figure 4.2 and consider a small element dx. The elastic wave passes through it in time dt = (dx)/c. The relationship between the longitudinal stress σ at any point in a body and the longitudinal velocity v at that point comes from *Newton's second law of motion*

$$Ft = mv \qquad \text{(Eqn 4.7)}$$

where F is the longitudinal force acting on a given cross section, t is the time the force acts, m is the mass it acts against, and v is the velocity imparted to m by F. Stated in differential form, Equation 4.7 becomes

$$Fdt = d(mv) \qquad \text{(Eqn 4.8)}$$

or

$$\sigma A dt = \rho A dx v \qquad \text{(Eqn 4.9)}$$

Since dt = (dx)/c,

$$\sigma A dt = \rho A c dt v \qquad \text{(Eqn 4.10)}$$

therefore

$$\sigma = \rho c v \qquad \text{(Eqn 4.11)}$$

where σ is the stress at any point in a disturbance, v is the particle velocity and c is the velocity of propagation of the wave disturbance [Ref. 11].

Elastic waves reflect at surfaces in a manner which depends on the boundary conditions at the surface. At a free end, a compressive pulse reflects as tension while at a fixed end it reflects as compression. To show this, we visualize a compressive pulse moving to the right and out of the rod as shown in Figure 4.4. In order to satisfy the boundary condition of zero stress (free end) we have to superimpose a tensile pulse moving into the rod from right to left as shown in Figure 4.5.

B. PHYSICS OF SPALLING

Consider a material which is strong in compression and which will fail in tension at some lower value of stress. In addition, consider a saw tooth compressive pulse, which is reasonably typical of explosions, whose maximum stress σ_o is greater than the tensile strength of the material. The pulse will advance toward the surface of the material and begin to be reflected as shown in Figure 4.5 the net stress at the front of the reflected pulse will be constantly changing and will be the algebraic sum of the tension and

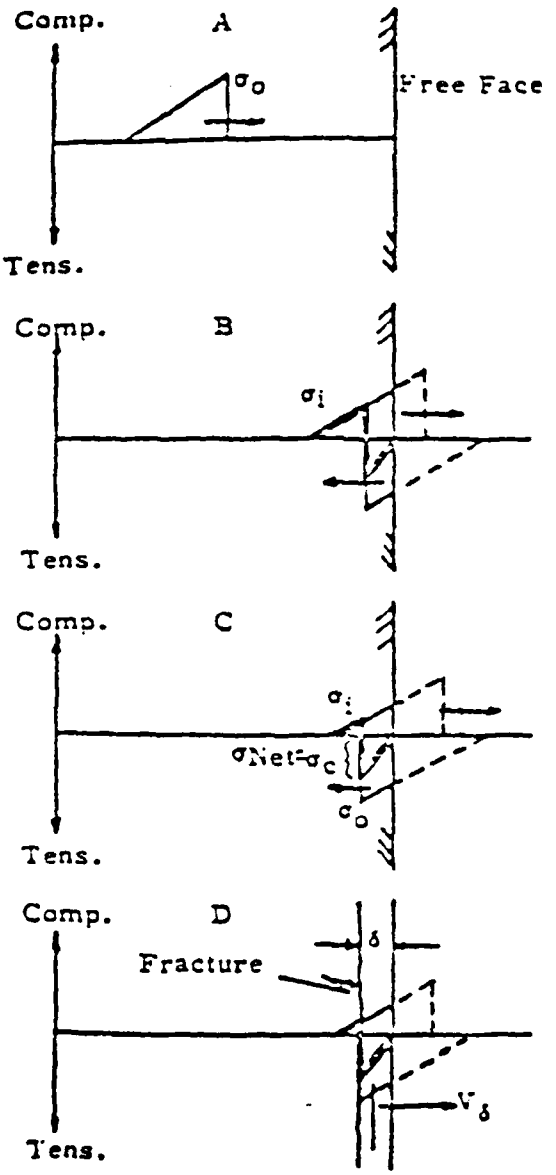

Figure 4.4 Reflection of Waves at a Free Surface [Ref. 12]

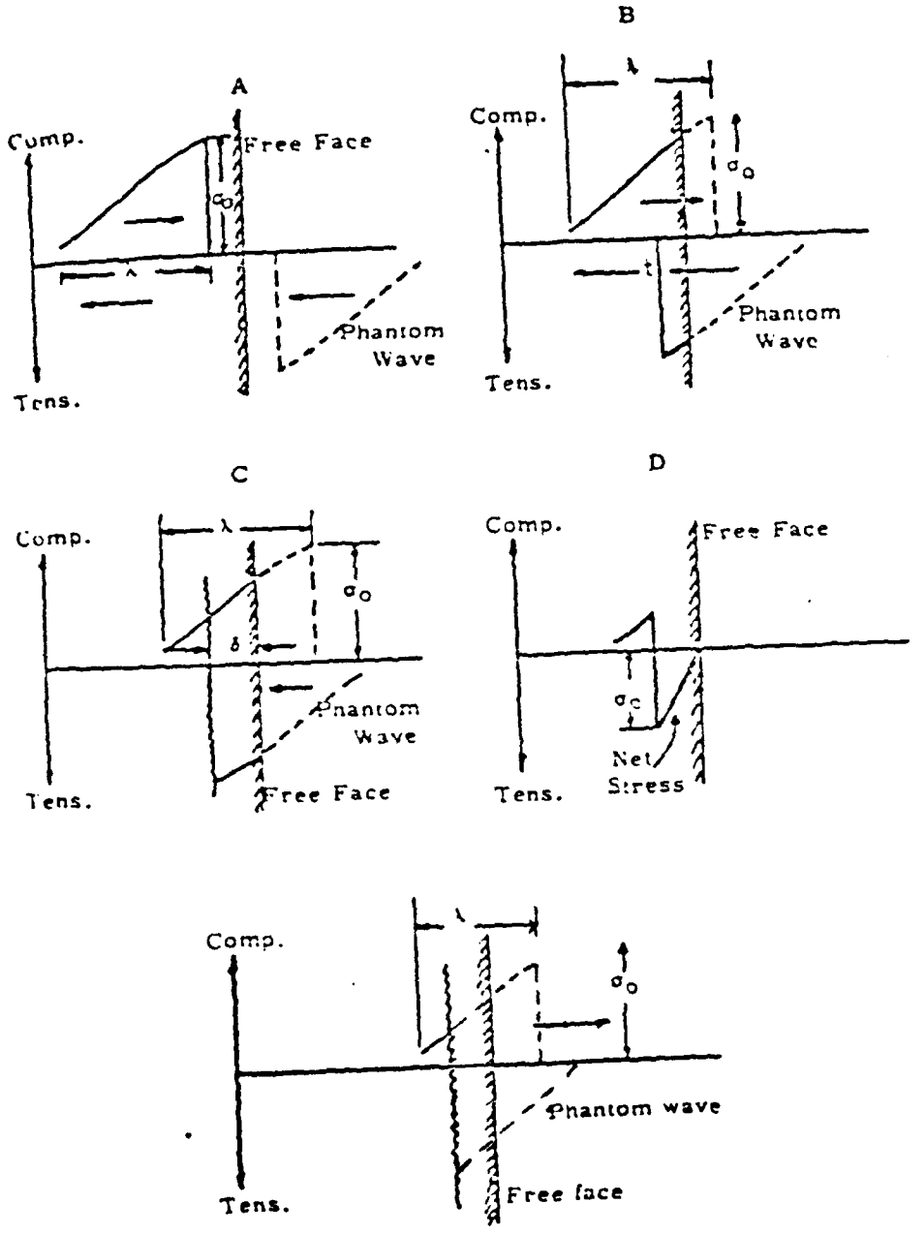

Figure 4.5 Dynamics of Spalling [Ref. 12]

compression at the point. If the compression acting at the same point as the front (and therefore maximum) of the tension is denoted as σ_i, then the net stress at the front of the reflected wave will be represented by the equation

$$\sigma_{net} = \sigma_i - \sigma_o \qquad \text{(Eqn 4.12)}$$

where a compressive stress is considered positive and a tension stress negative. From Figure 4.5 it can be seen that the net stress at the front of the reflected wave will increase in tension from zero as the reflection progresses. Then at some point during the interference of the incident and reflected pulses the net stress at the front of the reflected pulse will be equal to the critical normal stress σ_c necessary to fracture the material. Then

$$\sigma_c = \sigma_o - \sigma_i \qquad \text{(Eqn 4.13)}$$

and a fracture will form in the material at the position of the front of the reflected wave.

An amount of the initial wave between σ_o (the front) and σ_i is now trapped in the material between the initial surface and newly created fracture surface. The momentum of the trapped portion of the wave maintains a velocity in the direction of the initial pulse. This velocity can be found by equating the impulse of the trapped part of the wave to the momentum of that portion of the material

$$\rho \delta v = \frac{\sigma_o + \sigma_i}{2} t \qquad \text{(Eqn 4.14)}$$

where δ is the thickness of the separated material and t is the time between σ_o and σ_i [Ref. 12].

The formation of the fracture and separation of the fractured material from the original material is known as spalling and the newly created portion of material δ is known as spall.

It is possible to express the thickness δ and velocity v_s of the spall in terms of σ_o, σ_c and the length of the pulse λ, if these parameters and the shape of the pulse are known.

For single spalling,

$$\sigma_c = \sigma_o - \sigma_i \qquad \text{(Eqn 4.15)}$$

and from geometry, one obtains,

$$\sigma_i = \sigma_o \frac{\lambda - ct}{\lambda} \qquad \text{(Eqn 4.16)}$$

where λ is the length of the pulse and ct is the linear distance between σ_o and σ_i, since c is the velocity of propagation and t is the time between these two values. By close examination of the geometry of reflection it can be seen that

$$ct = 2\delta \qquad \text{(Eqn 4.17)}$$

where δ is the depth of thickness of spall. Then combine equations 4.15, 4.16 and 4.17 and solve for δ

$$\delta = \frac{\sigma_c}{\sigma_o} \frac{\lambda}{2} \qquad \text{(Eqn 4.18).}$$

To find the velocity of the spall v_s in terms of these known parameters substitute equations 4.15, 4.17 and 4.14 and solve for v_s

$$v_s = \frac{2\sigma_o - \sigma_c}{\rho c} \qquad \text{(Eqn 4.19)}$$

C. EFFECTS OF INTERFACES AND LAMINATIONS

When the physical properties of a medium which is transmitting a transient pulse change abruptly, the disturbance will be modified as it crosses this change, or interface. As we have seen, the pulse will be both reflected and transmitted.

A property of any medium which is of great importance when considering the transmission of a disturbance is its specific acoustic impedance ρc defined as the product of density times the velocity of propagation of transient stresses.

The laws which govern the modification of the pulse as it crosses the interface are derived from the two boundary conditions: (1) the stresses on the two sides of the interface are equal and (2) the particle velocities normal to the boundary are equal. The first condition results from the fundamental law of hydrostatic pressures and it can be shown that as long as normal incidence alone is considered, the condition must also hold for solids. The second condition

is equivalent to saying that the two media remain in constant contact at the boundary. These conditions must, of course, hold for every point on the incident wave.

The two equations which express the above conditions can be written as

$$\sigma_I + \sigma_R = \sigma_T \qquad \text{(Eqn 4.20)}$$

and

$$u_I + u_R = u_T \qquad \text{(Eqn 4.21)}$$

where σ_I, σ_R, σ_T, u_I, u_R, and u_T are the instantaneous values of stress and particle velocity, respectively, for the incident, reflected and transmitted pulses, respectively. These states are shown in Figure 4.6.

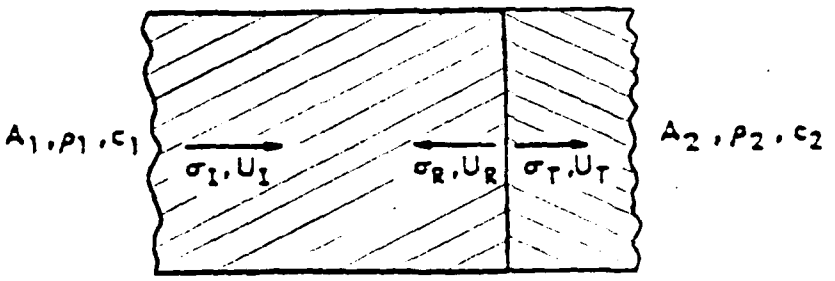

Figure 4.6 Interface Boundary Conditions

From equation 4.17 it follows

$$u_I = \frac{\sigma_I}{\rho_1 c_1} \qquad u_R = \frac{-\sigma_R}{\rho_1 c_1} \qquad u_T = \frac{\sigma_T}{\rho_2 c_2} \qquad \text{(Eqn 4.22)}$$

where ρ and c are the density of the material and velocity of propagation of the pulse, respectively, and subscripts denote the first and second mediums. Substituting equation 4.22 into 4.21

$$\frac{\sigma_I}{\rho_1 c_1} - \frac{\sigma_R}{\rho_1 c_1} = \frac{\sigma_T}{\rho_2 c_2} \qquad \text{(Eqn 4.23)}$$

and solving equations 4.20 and 4.23 simultaneously, first for σ_T in terms of σ_I, then for σ_R in terms of σ_I, the two fundamental equations governing the distribution of stress at an abrupt change in media will be obtained:

$$\sigma_T = \frac{2\rho_2 c_2}{\rho_2 c_2 + \rho_1 c_1} \sigma_I \qquad \text{(Eqn 4.24)}$$

$$\sigma_R = \frac{\rho_2 c_2 - \rho_1 c_1}{\rho_2 c_2 + \rho_1 c_1} \sigma_I \qquad \text{(Eqn 4.25)}$$

The above two equations have several inherent implications which are valuable aids in understanding why and how the pulse is modified at an interface. A brief and elegant examination of this phenomenon can be accomplished by dividing equation 4.25 by equation 4.24 to obtain a ratio of the stress reflected to the stress transmitted

$$\frac{\sigma_R}{\sigma_T} = \frac{\rho_2 c_2 - \rho_1 c_1}{2\rho_2 c_2} \qquad \text{(Eqn 4.26)}$$

From this expression it can be seen immediately that when $\rho_2 c_2$ is approximately equal to $\rho_1 c_1$ nearly all of the stress is transmitted, whereas if $\rho_2 c_2$ differs greatly from $\rho_1 c_1$ most of the stress is reflected at the boundary.

D. ANALYSIS OF TEST DATA VS. THEORETICAL RESULTS

The permanent deformations of the 5083 aluminum plate are shown in Figure 2.4 and the spall phenomenon agrees well with the theoretical studies. In particular, when the aluminum plate was subjected to the shaped charge without the kevlar liner in direct contact with the back of the plate (free surface condition--shot #3), the magnitude of the tension stress is approximately 8.65E06 psi as calculated by equation 4.25 where $\rho_1 c_1$ was approximately equal to 8.35E04 (lbf-sec)/ft^3, $\rho_2 c_2$ was approximately equal to 2.66 (lbf-sec)/ft^3 and the incident stress was approximately equal to 8.65E06 psi. The depth of spall for this configuration was physically measured to be approximately 0.47 inches. However when the kevlar liner was placed in direct contact with the back of the aluminum plate (shot #2), the magnitude of the stress as calculated by equation 4.25 is approximately 7.53E04 psi where $\rho_1 c_1$ was the same value as before, $\rho_2 c_2$ was approximately equal to 8.50E04 (lbf-sec)/ft^3

and the incident stress was also the same value as before. In this case the spall depth was approximately 0.28 inches.

The principle for total elimination of spallation for a target perforated by a shaped charge jet is embodied in an armor system composed of layers of materials having different thicknesses and specific impedances. Therefore for certain jet impact conditions, the reflected shock wave strength at the interior surface of the target is less than or equal to the dynamic strength of the material at the interface. Under these conditions, the target material will not spall, even though the jet perforates the target. Hence by making use of only the fundamental equations it is possible to decrease the stress of a pulse by the use of an extended series of materials, each material of decreasing specific acoustic impedance.

As previously mentioned, the second objective for this study was to attempt to measure and record transient strains during the shock loading. For this case of impulsive loading conditions, the plastic deformation is supposed to be brought about by bending stresses only and thus combined bending and tension is not analytically considered. In essence, when the plate deflection and deformation is significant the plate experiences in-plane stretching due to the outstanding bending stresses. Therefore the strain gages attached to the panel were designed to measure transient strains in the radial and tangential directions of the

plate. These strains in turn would be converted to stresses according to the relationship:

$$\sigma_R = \frac{E}{1 - \nu^2} (\varepsilon_r + \nu\varepsilon_\theta) \qquad \text{(Eqn 4.27)}$$

However in calculating the magnitude of these stresses using the data from the strain traces of the events, it becomes obvious that the impulse signal did seem to overload the Honeywell recorder because the stresses are significantly smaller than expected. This notable discrepancy between expected derived values of stress and experimentally obtained values of stress indicates that the strain traces are not valid throughout the recorded time period.

Although the calibration shot appeared to successfully bracket and capture the transient strain data as viewed through an on site oscilloscope (and verified by an electronics technician), it remains essential to confirm this calibration information prior to continuing with the test project. Despite the fact that the material characterization is incomplete, further shaped charge shots could not be performed in the present effort because of fund limitations.

V. CONCLUSIONS AND RECOMMENDATIONS

The spall suppression effect of kevlar in intimate contact and spaced configuration with 5083 aluminum armor plating were investigated. The shaped charges were statically detonated at an 8 inch standoff from the targets. The spall depths on these plates were taken as a measure of the potential lethality of the attack.

It was found that the presence of the kevlar liner in intimate contact with the 5083 aluminum panel significantly reduced the depth of spall for the 3.2 inch BRL precision shaped charge compared to the spall depth of the aluminum panel backed with spaced kevlar. In addition, it is recognized that the shaped charge jet penetration is basically unaltered by the addition of the liner; the primary function of the kevlar liner is spall and associated fragment suppression.

Behind armor effects can be suppressed from shaped charge attack by making use of only the fundamental equations established in chapter 4. In particular, it is possible to decrease the stress of a shock pulse by the use of an extended series of materials or laminations, each material of decreasing specific acoustic impedance. The major disadvantage of this method is the limited number of materials with sufficiently specific acoustic impedances

not to mention the practicality and feasibility of manufacturing such an armor system for armored fighting vehicles.

Tests of spaced armor liners have proven effective in reducing the size of the debris cone angle and in capturing up to 90% of all the spall that occurs after a shaped charge attack. However, a more effective means of spall suppression is to attach the spall liner system directly to the back side of the armor plating.

The second objective of the present study was to obtain high quality transient strain data for the aluminum panel subjected to the shaped charge impact. Unfortunately transient strain traces obtained were not valid over as long as time as desired because the gages in that region became detached during the transient response. In addition, it is believed that the response signal was far in excess of the capabilities of the present available recording devices. Hence further test shots are needed and recommended to characterize the material condition at tensile failure. In this regard, once this data is confirmed, it is believed to be essential in providing information to permit rational predictions of spall in aluminum panels which have been subjected to impulsive loading conditions.

APPENDIX A

TABLES AND FIGURES

TABLE A.1

FIRING SEQUENCE

SHOT #	CONDITIONS
PLATE 1	24" X 24" 5083 ALUMINUM MOUNTED WITH THREE STRAIN GAGE ROSETTES FOR CALIBRATION
PLATE 2	ALUMINUM PLATE WITH KEVLAR LINER IN DIRECT CONTACT TO BACK SURFACE (3 STRAIN ROSETTES)
PLATE 3	ALUMINUM PLATE WITH KEVLAR LINER SPACED 8" FROM BACK SURFACE (3 STRAIN GAGE ROSETTES)

TABLE A.2

STRAIN GAGE LOCATIONS

STRAIN GAGE ID NUMBER	LOCATION			
	X(in.)	Y(in.)	DIRECTION OF STRAIN MEASUREMENT	ORIENTATION θ(deg) a
1	2.828	-2.828	RADIAL	315
2	2.828	-2.828	RADIAL	315
3	-2.828	-2.828	TANGENTIAL	225
4	-2.828	-2.828	TANGENTIAL	225
5 b	-2.828	-2.828	RADIAL	225
6 b	-2.828	-2.828	TANGENTIAL	225

a: see fig. A.1 for definition of θ

b: denotes strain gages were mounted on back surface

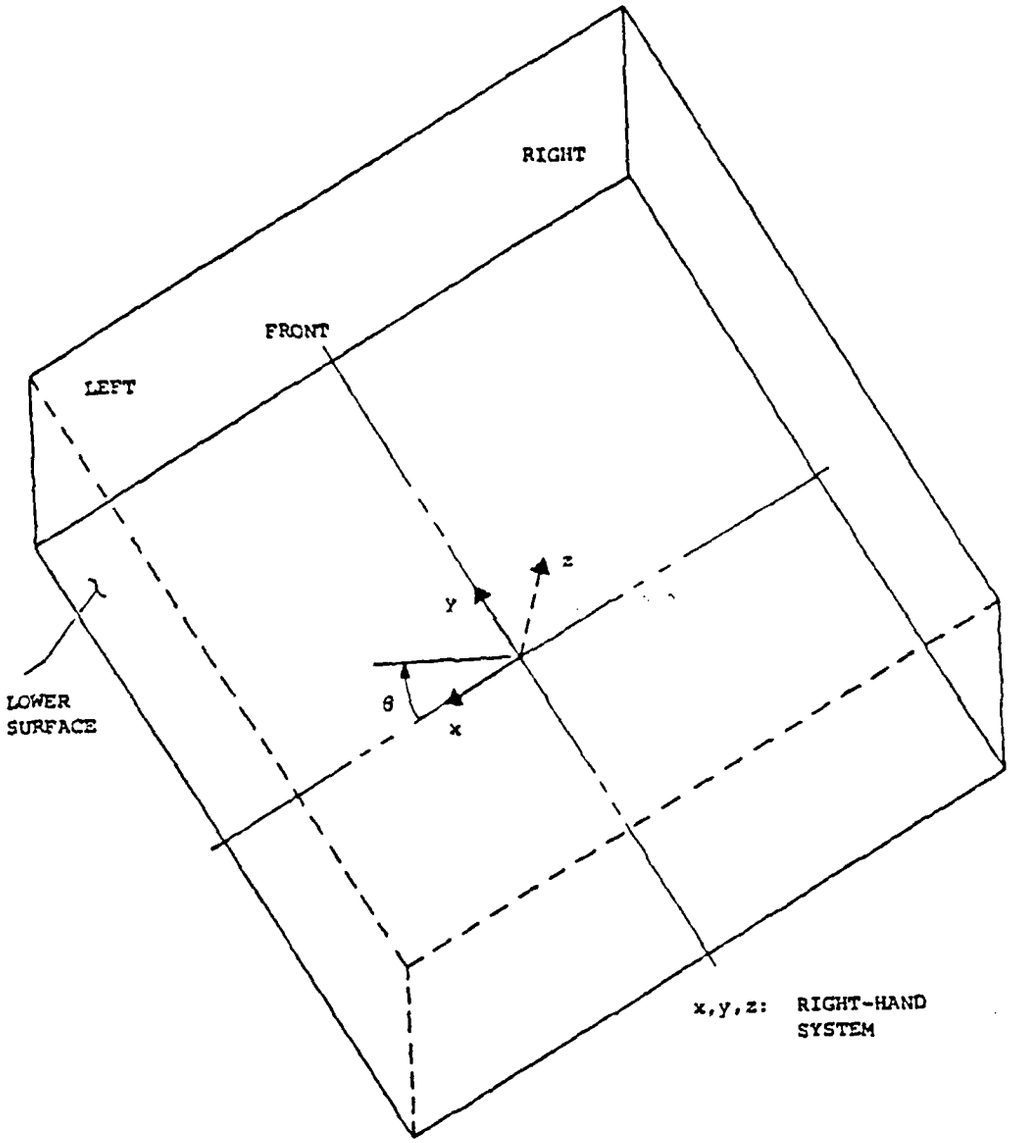

FIG. A.1 PANEL MODEL COORDINATES AND NOMENCLATURE

LIST OF REFERENCES

1. Backofen, J. E., "Tank-War Machine for Land Combat," Armor, January-February, pp. 10-12, 1980.

2. Roecker, E. T., Spall Ring Diameter and Paths of Peripheral Spall Particles from Shaped Charge Jet Perforation of Armor Plate, BRL Memorandum Report No. 2788, September 1976.

3. Office of Scientific Research and Development, Effects of Impact and Explosion, Summary Technical Report of Division 2 (NDRC), 1946.

4. Ogorkiewixz, R. M., "The Next Generation of Battle Tanks," International Defense Review, Special Series, Battle Tanks, pp. 48-52, 1976.

5. Goldsmith, W., Impact, Edward Arnold (publishers) Ltd., 1960.

6. O'Brien, J. L. and Davis, R. S., "On the Fracture of Solids Under Impulsive Loading Conditions," Response of Metals to High Velocity Deformation, New York, 1960.

7. Backofen, J. E., "Armor Technology Part III," Armor, March-April, 1983.

8. Kennedy, D. R., "Improving Combat Crew Survivability," Armor, July-August, 1983.

9. Ibid., pp. 16-22.

10. Thomson, W. T., Theory of Vibrations with Applications, Prentice-Hall, Inc., New Jersey, 1981.

11. Zukas, J. A., Nicholas, T., Swift, H. F., Greszczuk, L. B., and Curran, D. R., Impact Dynamics, John Wiley and Sons, New York, 1982.

12. Rinehart, J. S., On Fractures Caused by Explosions and Impacts, Colorado School of Mines, 1960.

INITIAL DISTRIBUTION LIST

		No. Copies
1.	Defense Technical Information Center Cameron Station Alexandria, Virginia 22314	2
2.	Library, Code 0142 Naval Postgraduate School Monterey, California 93943	2
3.	Department Chairman, Code 69 Department of Mechanical Engineering Naval Postgraduate School Monterey, California 93943	1
4.	Professor Y. S. Shin, Code 69 Department of Mechanical Engineering Naval Postgraduate School Monterey, California 93943	7
5.	Professor R. E. Newton, Code 69 Department of Mechanical Engineering Naval Postgraduate School Monterey, California 93943	1
6.	Colonel Robert M. Wilson c/o Department of Mechanics United States Military Academy West Point, New York 10996	1
7.	Colonel David H. Cameron Department Head--Department of Mathematics United States Military Academy West Point, New York 10996	1
8.	Mr. R. E. Musante Manager, Armor Design Group Ordnance Division FMC Corporation California 90041 1105 Coleman Ave., Box 1201 San Jose, California 95108	1

9. Mr. A. P. Lee — 1
Ordnance Division
FMC Corporation California 90041
1105 Coleman Ave.
San Jose, California 95108

10. Captain M. K. Asada — 5
120 Old Deerfield Pike
Bridgeton, New Jersey 08302

11. Colonel T. M. Montgomery — 1
HQ 21st SPT CMD
Attention: AEIRG
APO New York, New York 09325


ATE
LMED